nature mental health

Article

https://doi.org/10.1038/s44220-024-00286-2

Deep brain stimulation of habenula reduces depressive symptoms and modulates brain activities in treatment-resistant depression

Received: 2 September 2023

Accepted: 16 May 2024

Published online: 12 July 2024

Check for updates

Zhiyan Wang[1,2,3], Chao Jiang[4], Lingxiao Guan[3], Lei Zhao[1,2], Tengteng Fan[5], Jian Wang[4], Xiaodong Cai[6], Yingli Zhang[7], Chen Yao[6], Bo Peng[7], Feixue Wang[1,2], Chunhua Hu[3], Zhiqiang Cui[4] ✉, Yiheng Tu[1,2] ✉ & Luming Li[3,8] ✉

The habenula (Hb) is a phylogenetically old structure connecting forebrain and brainstem monoaminergic nuclei that has been implicated in the pathogenesis of depression. Here, to investigate the clinical efficacy and neural mechanisms of stimulating the Hb for alleviating depression symptoms in humans, we bilaterally implanted electrodes in six patients with treatment-resistant depression and delivered high-frequency stimulation. Compared to baseline, we observed a substantial reduction in Hamilton Depression Rating Scale scores: 62.1% at 1-month, 64.0% at 3-month and 66.2% at 6-month follow-up. Local field potential data showed that acute Hb stimulation increased theta-band power, especially in the right side, which was related to the following clinical remission. Moreover, functional magnetic resonance imaging data showed that acute Hb stimulation enhanced blood oxygen level-dependent responses of the medial orbitofrontal cortex, raphe and substantia nigra, which are important components of the dopaminergic and serotonergic systems. Our findings demonstrated that Hb stimulation can alleviate depressive symptoms and modulate the activity of the medial orbitofrontal cortex, raphe and substantia nigra in treatment-resistant depression patients. This trial was registered under the clinical trial numbers NCT03667872 and ChiCTR2100045363.

Major depressive disorder (MDD) is a leading cause of disability and mortality worldwide. Approximately 30% of patients failed to respond to standard therapies (for example, antidepressant medication and psychotherapy), resulting in treatment-resistant depression (TRD)[1]. Deep brain stimulation (DBS), which involves the implantation of electrodes in specific regions of the brain and the delivery of electrical impulses to modulate neural activity, has emerged as a promising treatment for MDD. Several brain regions have been targeted for relieving depressive symptoms, including the subcallosal cingulate cortex (SCC), nucleus accumbens (NAc), the anterior limb of the internal capsule and the medial forebrain bundle (MFB)[1,2]. However, results from randomized controlled trials were not consistently replicated[3–6]. Although the inconsistency may arise from several factors, including the heterogeneity of the patient population, the complexity of the disorder and the variability of the surgical procedures and stimulation parameters, the low response rates suggest novel targets in DBS treatment are needed[7].

The habenula (Hb) has recently emerged as a potential therapeutic target for depression[8,9], supported by evidence from human and animal

A full list of affiliations appears at the end of the paper. ✉e-mail: zhiqiangcui2008@hotmail.com; yihengtu@gmail.com; lilm@tsinghua.edu.cn

https://doi.org/10.1038/s44220-024-00286-2

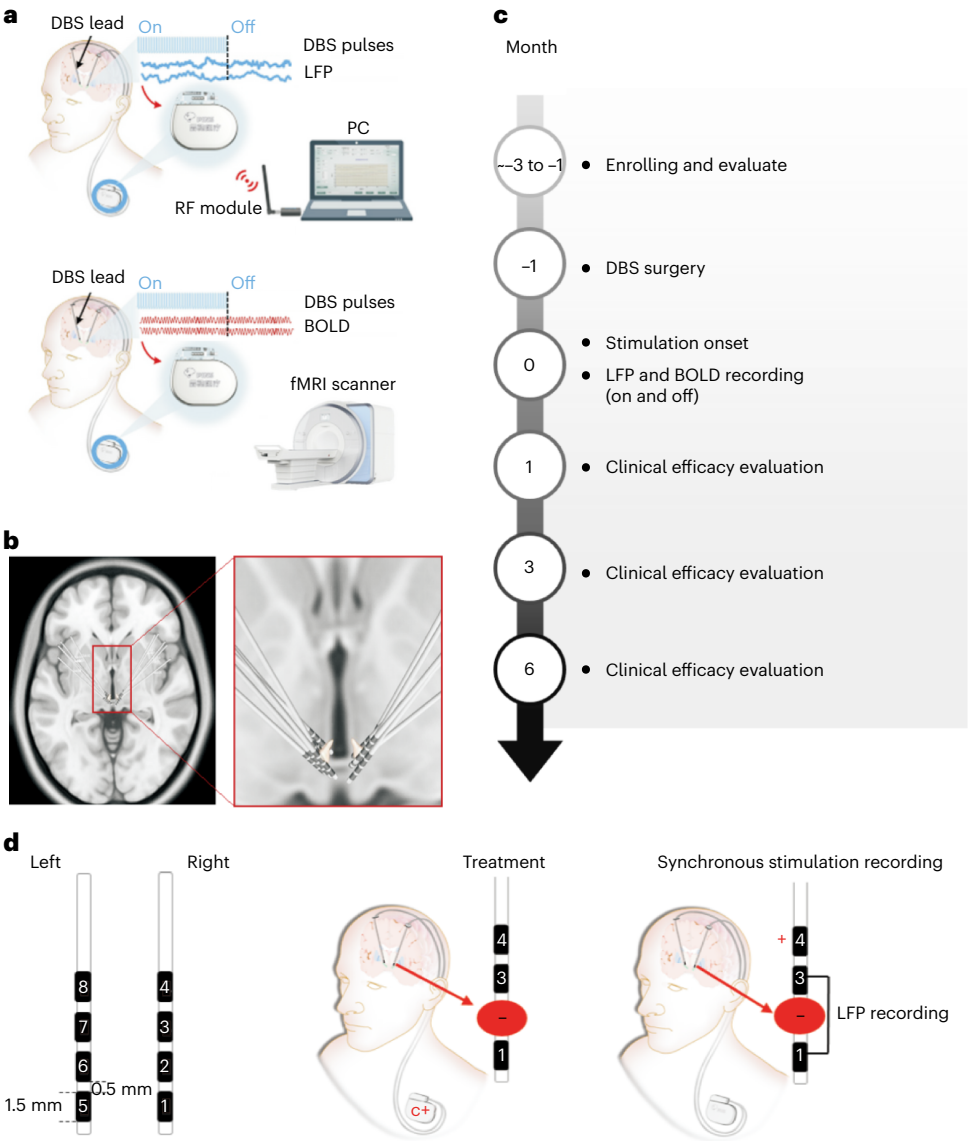

Fig. 1 | Equipment and experimental protocol. a, LFPs were recorded by the sensing-enabled neurostimulator and transmitted in real-time to the personal computer (PC) during on and off states; fMRI BOLD signals were also collected during on and off states. **b**, DBS electrodes locations in each patient. **c**, Clinical data collection and assessment procedure. **d**, A schematic diagram of DBS electrodes and contacts (left), an example of contacts for monopolar stimulation (middle) and LFP recording (right). RF, radio frequency.

studies linking Hb (especially the lateral nuclei, LHb) with multiple psychiatric disorders, particularly MDD[10–12]. Anatomically, the LHb exerts a powerful influence on downstream dopaminergic and serotonergic systems, including the ventral tegmental area (VTA), substantia nigra pars compacta (SNc) and raphe nucleus[13–15]. These monoaminergic centers send direct and indirect projections to the extensive cortical areas such as the orbitofrontal cortex (OFC)[16,17]. Functionally, the LHb serves as a major player and center of an antireward system, and aberrant activity in the LHb and its neural circuits has been implicated in the pathophysiology of depression[18,19].

Animal models of depression consistently show that the LHb exhibits enhanced activity and an increased number of burst-firing neurons[20]. Functional and structural imaging studies in humans also reveal hyperactivity and increased volumes in the Hb in individuals with MDD[21,22]. Building on the successful use of high-frequency stimulation to block hyperactivity in the subthalamic nucleus in Parkinson's disease, recent pilot studies have evaluated the safety and efficacy of high-frequency Hb DBS in patients with TRD[23,24], suggesting Hb as a promising target for DBS in depression. However, the mechanisms by which high-frequency stimulation modulates Hb activity and neural circuits, as well as its association with depressive symptoms in patients, are currently unknown.

In this Article, we conducted an open-label clinical trial and implanted electrodes into the Hb of six TRD patients. The DBS system enabled wireless collection of local field potential (LFP) signals during both on- and off-stimulation periods and was compatible with magnetic resonance imaging (MRI) (Fig. 1a). We collected LFP signals from bilateral Hb as well as the whole-brain blood oxygen level-dependent (BOLD) signals during turning stimulation on and off at the first treatment session (defined as month 0), and tracked clinical outcomes at 1-, 3- and 6- month follow-ups (Fig. 1c). We investigated the acute LFP/BOLD responses induced by Hb DBS and examined the associations between brain responses and clinical improvements.

Results

Patient information

Six patients with TRD (five unipolar and one bipolar) were enrolled in this study. Their demographic and clinical characteristics are presented

https://doi.org/10.1038/s44220-024-00286-2

Table 1 | Patient demographic and clinical information

Patient	1	2	3	4	5	6	Group
Gender	M	F	M	F	F	F	4 female (F)/ 2 male (M)
Current age	34	30	22	34	18	22	26.67±6.89
Age at MDD onset	13	8	16	32	13	15	16.17±8.23
Past ECT	Yes	Yes	Yes	Yes	No	Yes	5 of 6
Past psychotherapy	Yes	Yes	Yes	Yes	Yes	Yes	6 of 6
Past TMS	No	Yes	Yes	No	Yes	No	3 of 3
Past ketamine	Yes	No	No	No	No	No	1 of 6
DSM-5 diagnosis	UP	UP	UP	UP	BP	UP	5 UP/1 BP
$HDRS_{17}$	22	35	27	30	25	35	29.00±5.33
HARS	20	46	21	25	33	33	29.67±9.79
Number of preoperative medications	3	4	3	5	5	1	3.5±1.52

ECT, electroconvulsive therapy; TMS, transcranial magnetic stimulation; DSM-5, Diagnostic and Statistical Manual of Mental Disorders, 5th Edition; UP, unipolar; BP, bipolar.

in Table 1. The patients underwent bilateral Hb DBS surgery between January 2019 and March 2022. They had an average age of 26.67 (ranging from 18 to 34) years and were mostly female ($n = 4$). Their baseline average score on the 17-item Hamilton Depression Rating Scale ($HDRS_{17}$) was 29.00 (ranging from 22 to 35) and their average age of MDD onset was 16.17 (ranging from 8 to 32) years. At baseline, they were taking an average of 3.5 medications (ranging from 1 to 5), which are listed in Supplementary Table 2.

Clinical outcomes

At the individual level, DBS electrodes were precisely implanted into the bilateral Hb (Fig. 1b and Supplementary Fig. 1). Patients received continuous monopolar stimulation (an example is shown in Fig. 1d) with individualized therapeutic voltage (the pulse and frequency were fixed at 90 μs and 160 Hz) throughout the six-month treatment. Details of the individualized therapeutic contact and parameters can be found in Supplementary Table 1. The volume of tissue activated with the initial treatment parameters are shown in Supplementary Fig. 1. Notably, patient 6 withdrew from the study at the 3-month follow-up due to a personal choice of discontinuing further follow-ups. Thus, data from five patients were analyzed for both the 3- and 6-month follow-up evaluations.

Compared to baseline, the $HDRS_{17}$ score in the six patients was reduced by 62.1% at 1-month follow-up (29.0 ± 5.3 versus 11.0 ± 8.1, $P = 0.03$), 64.0% at 3-month follow-up (27.8 ± 5.0 versus 10.0 ± 4.4, $P = 0.06$) and 66.2% at 6-month follow-up (27.8 ± 5.0 versus 9.4 ± 5.0, $P = 0.06$) (Fig. 2a). The number of clinical responders ($HDRS_{17}$ score reduction ≥50% from baseline) was 5, 5 and 3 at 1-, 3- and 6-month follow-up, respectively. The number of clinical remission ($HDRS_{17}$ score <8) was 2, 1 and 1 at 1-, 3- and 6-month follow-up, respectively. Patient 4 achieved remission in all follow-ups. The Hamilton Anxiety Rating Scale (HARS) score was reduced by 59.6% at 1-month follow-up (29.7 ± 9.8 versus 12.0 ± 8.9, $P = 0.03$), 64.1% at 3-month follow-up (29.0 ± 10.8 versus 10.4 ± 7.4, $P = 0.06$) and 64.1% at 6-month follow-up (29.0 ± 10.8 versus 10.4 ± 8.2, $P = 0.06$) (Fig. 2b).

At the 1-month follow-up, the number of medications used in the six patients remained the same as at baseline, ranging from one to five. However, excluding patient 6, the number of medications used by the remaining five patients decreased from 4.00 (ranging from 3 to 5) at baseline to 3.60 (ranging from 1 to 5) and 2.60 (ranging from 1 to 4) at the 3- and 6-month follow-up, respectively. Supplementary Table 2 provides details of individualized medication use.

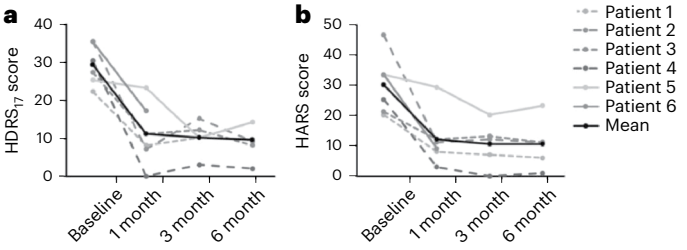

Fig. 2 | Individualized clinical outcomes. a, The $HDRS_{17}$ score of each patient at baseline, 1-, 3- and 6-month follow-up. **b**, The HARS of each patient at baseline, 1-, 3- and 6-month follow-up.

No surgery-, device- or disease-related complications were reported during the perioperative period, as reported in our previous studies[25,26]. Four patients reported instantaneous electrical sensation and one patient reported dizziness upon initial activation of the DBS, which quickly subsided. No other surgery-, device- or disease-related adverse events were observed throughout the 6-month treatment.

Outcomes of LFP in the Hb

To investigate the effects of high-frequency (160 Hz) stimulation of Hb on its neural activities, we recorded the LFP of bilateral Hb with DBS turned off and on at month 0. The LFP of patient 1 was excluded from the analysis because of the short data duration with DBS on. Thus, LFP data from five patients were analyzed at month 0.

The bipolar stimulation and LFP recording contacts (an example is shown in Fig. 1d) for each patient are listed in Supplementary Table 3. The power spectral density (PSD) of different frequency bands in the right and left Hb during DBS 'off' and 'on' are illustrated in Fig. 3a,b, respectively. After the DBS was turned on, the power of the theta band in right Hb increased in all patients (0.23 ± 0.05 versus 0.26 ± 0.06, $P = 0.06$; Fig. 3a). In contrast, although the power of the theta band in left Hb also increased at the cohort level (0.22 ± 0.04 versus 0.27 ± 0.04, $P = 0.13$; Fig. 3b), it showed inconsistent changes across patients. The power of the delta, alpha and beta bands in both the right and left Hb showed no notable difference at the cohort level and inconsistent changes across patients (Fig. 3a,b). Individual values are provided in Supplementary Table 4.

We then provide individual data showing changes in theta-band PSD and changes in $HDRS_{17}$ at 1-, 3- and 6-month follow-ups (Fig. 3c,d). These data demonstrated that patients who achieved remission at all follow-up sessions had a greater increase in theta-band PSD in the right but not left Hb at month 0 (Fig. 3c,d). These results suggested that the higher theta-band PSD response to acute stimulation in the right Hb was related to clinical remission.

Outcomes of BOLD in the reward system

To investigate the effects of high-frequency stimulation of Hb on the reward system, we examined the fractional amplitude of low-frequency fluctuation (fALFF) when turning DBS off and on at month 0 (Fig. 1c). The results showed that the fALFF of the medial orbital gyrus (mOFC), raphe nucleus and SNc were significantly and consistently increased after DBS activation (mOFC: 0.575 ± 0.015 versus 0.585 ± 0.014, $P = 0.03$; Fig. 4a; raphe nucleus: 0.558 ± 0.024 versus 0.579 ± 0.023, $P = 0.03$; Fig. 4b; and SNc: 0.556 ± 0.008 versus 0.571 ± 0.015, $P = 0.03$; Fig. 4c). However, the fALFF of other core components of the reward system including lateral OFC, putamen, NAc and VTA, did not show significant changes at the cohort level, nor did they show consistent changes at the individual level after DBS was turned on (Supplementary Table 5 and Supplementary Fig. 2).

Discussion

In this prospective open-label clinical study, we aimed to investigate the clinical efficacy and neural mechanisms of Hb DBS in patients with

https://doi.org/10.1038/s44220-024-00286-2

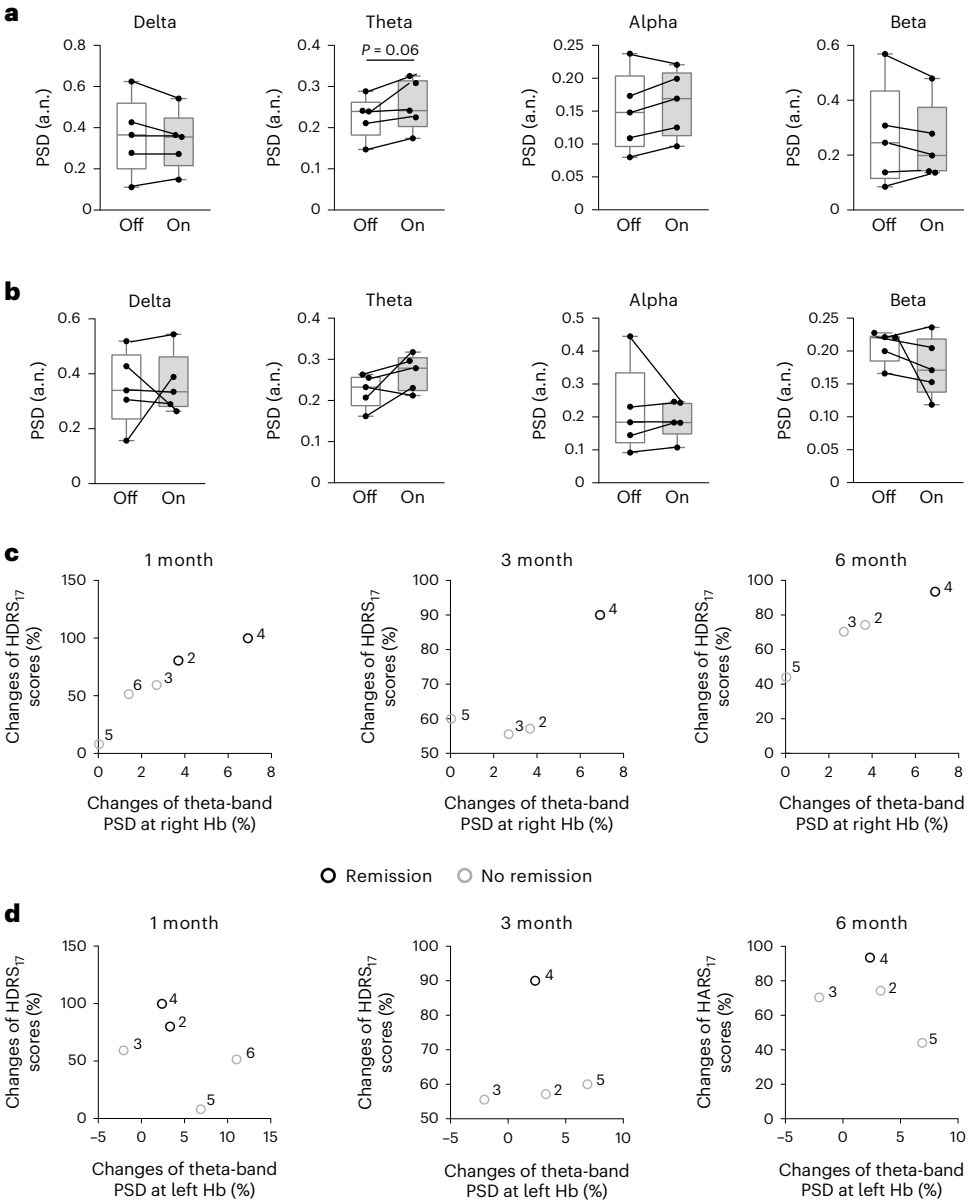

Fig. 3 | The modulation of PSD at the Hb by acute stimulation and its relationship with clinical improvements. a, PSD changes from five patients in different bands (delta, theta, alpha and beta) in right Hb after DBS activation. The center line indicates the mean, the bottom and top edge of the box indicates the 25th and 75th percentiles and the whiskers indicate the minimum and maximum, respectively. Only the power of the theta band in the right Hb increased in all patients (two-sided Wilcoxon matched-paired signed rank test, $W = 15$, $P = 0.06$). **b**, PSD changes from five patients in different bands (delta, theta, alpha and beta) in left Hb after turning DBS on. The center line indicates the mean, the bottom and top edge of the box indicates the 25th and 75th percentiles and the whiskers indicate the minimum and maximum, respectively. **c**, Individual data showed that patients who achieved remission at 1-, 3- and 6-month follow-ups had a greater increase in theta-band PSD in right Hb at month 0. **d**, Individual data showed that patients who achieved remission at 1-, 3- and 6-month follow-ups had no relation to the theta-band PSD in left Hb at month 0. a.n., normalized.

TRD. All six patients who received 160 Hz Hb DBS showed improvements in depressive symptoms, with an average reduction of 62.1% at 1-month follow-up ($n = 6$), 65.5% at 3-month follow-up ($n = 5$) and 67.6% at 6-month follow-up ($n = 5$). Similarly, anxiety symptoms also decreased, with an average reduction of 59.6% at 1-month, 65.0% at 3-month and 65.0% at 6-month follow-up. These clinical improvements were consistent with our initial case study[25] and another recently reported study, which demonstrated that chronic Hb DBS treatment resulted in a rapid and sustained improvement in depression, comorbid anxiety symptoms, sleep quality, health status and functional impairments[24]. Taken together, these results provide strong support for the clinical benefits of high-frequency Hb DBS for patients with TRD. In addition, at 1 or 3 months, the response/remitter rates are comparable or even superior to those reported with DBS targeting the MFB or SCC. However, at 6 months, the response/remitter rates appear to be similar or potentially lower compared to DBS targeting the MFB or SCC[9,24,27,28]. These findings suggested that the Hb could be a promising target for DBS in the treatment of TRD, similar to the MFB or SCC.

It is worth noting that patients 2 and 5 stopped responding at 6 months, reflecting the fluctuations in clinical efficacy of Hb DBS over time, which have also been observed in DBS targeting MFB or SCC[27,28]. There are two potential reasons for the fluctuation in $HDRS_{17}$ scores among these patients. First, changes in the medication regimen may have contributed to the fluctuations in their $HDRS_{17}$ scores. For example, patient 2 transitioned from taking four medications to two, while patient 5 reduced the medication intake from five to two

https://doi.org/10.1038/s44220-024-00286-2

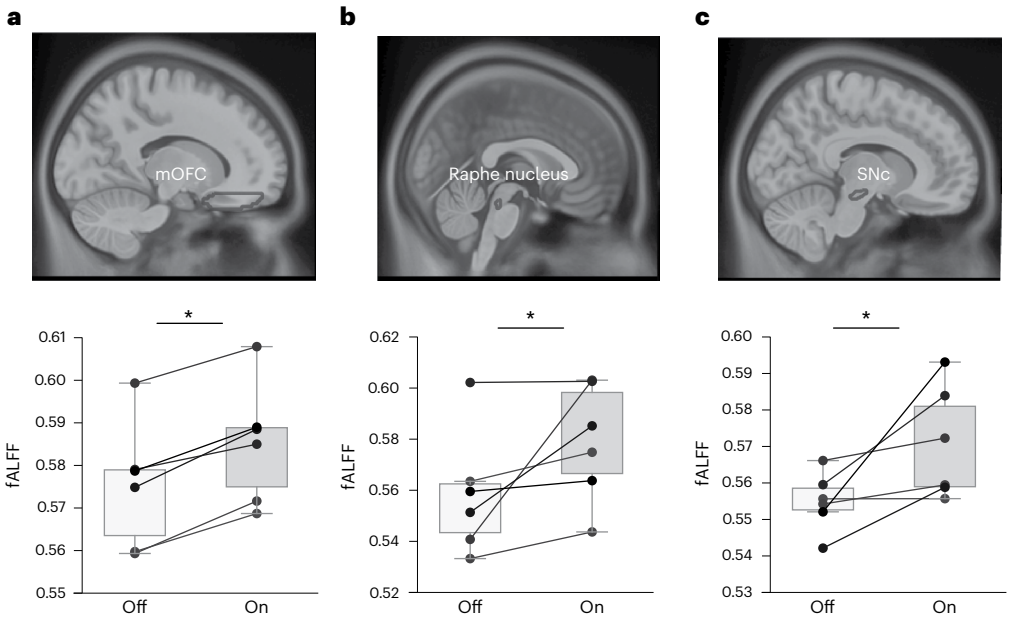

Fig. 4 | Acute stimulation induced fALFF changes in key regions of the reward system at month 0. a–**c**, Significant activation from six patients in the mOFC (**a**), the raphe (**b**) and the SNc (**c**) (two-sided Wilcoxon matched-paired signed rank test. mOFC: $W = 21$, $P = 0.0313$; raphe nucleus: $W = 21$, $P = 0.0313$; SNc: $W = 21$, $P = 0.0313$). The bottom and top edge of the box indicates the 25th and 75th percentiles, respectively. The whiskers indicate 1.5× the interquartile range up to the minimum and maximum. *$P < 0.05$.

between the 3-month and 6-month assessments. This adjustment in medication could have influenced their response to treatment. Second, it is important to note that the $HDRS_{17}$ scores primarily evaluate the patient's condition over the past 2 weeks and may be influenced by their current state at the time of assessment. Various factors, such as situational circumstances or temporary changes in mood, may impact the $HDRS_{17}$ scores at a specific assessment point.

Although a recent study showed that high-frequency DBS could reduce LHb burst firing but not the mean firing rate to ameliorate depression-like behaviors in rats[29], the electrophysiological evidence for Hb DBS in humans is lacking. In contrast to animal studies that recorded rapid synchronized firing of a group of neurons, our study collected LFP, which measures the summed electrical activity of a population of neurons. We reported that high-frequency stimulation increased the theta-band power of Hb, which was consistent with our first case report[25]. Our study is the first to determine the specific neural oscillation response to acute Hb DBS in humans with depression at the cohort level.

We found that the right theta-band activity increased in all patients after turning on stimulation, but not the left side, suggesting an asymmetric response of Hb DBS in TRD patients. This asymmetry has been observed in many animal studies showing left–right differences in Hb size and neural circuitry[30]. Similarly, human studies also showed the asymmetric function (that is, robust responses to the value of shock cues in the right Hb)[31] or structure (that is, larger in the left Hb)[32] in the left and right Hb, in both healthy participants and patients with MDD[33]. In addition, a recent study showed a strong negative correlation between patients' theta-band PSD from the right Hb and the severity of depression[24]. These results in patients also supported our findings that increased Hb theta-band power may reduce depressive symptoms. More importantly, our results found that a higher theta-band PSD response to acute stimulation in the patients' right Hb were related to clinical remission at all follow-ups. This is an interesting point, suggesting that Hb electrophysiology may potentially have some connection with treatment responses and need further investigation.

Rodent studies have shown that the Hb is functionally connected to other brain regions that regulates emotion[15,34–36]. A recent study with LHb DBS for two rat models of depression demonstrated that the activation of the limbic system and the monoaminergic systems played a critical role in the rapid antidepressant effects[37]. Our study is the first to demonstrate that high-frequency Hb stimulation increased brain activities in the mOFC, raphe nucleus and SNc, indicating that DBS can enhance synchronized activities in the part of reward system in TRD patients. This finding is consistent with previous research showing that DBS can modulate local neural activity and lead to changes in brain networks and behavioral outcomes[38,39].

Our study has several limitations. First, the sample size was small, and additional experiments are required to validate the findings regarding neural responses. Second, Although Hb electrophysiology might potentially be related to treatment responses, this needs to be confirmed in more long-term follow-ups. Further research is necessary to gain deeper insights into the neural mechanisms underlying these effects and to confirm one or more objective biomarkers to track recovery or relapse of depression and aid in optimizing treatment strategies.

Conclusions

Our study provides direct evidence that Hb stimulation can alleviate depressive symptoms and modulate the mOFC, raphe nucleus and SNc in patients with TRD. Larger and well-controlled clinical trials are needed to further validate the efficacy and neural mechanisms of Hb DBS for TRD.

Methods

Inclusion and exclusion criteria

This study included six patients with TRD who met the following inclusion criteria: (1) age between 18 and 70 years; (2) meeting the Diagnostic and Statistical Manual of Mental Disorders, 5th Edition (DSM-5) criteria for MDD or bipolar disorder, with a chronic illness episode lasting more than 1 year; (3) failure to respond to at least two adequate antidepressant medications from different classes, not including other therapies, such as psychotherapy or electroconvulsive therapy; (4) the $HDRS_{17}$ score ≥20 at each of two separate baseline visits (4–6 weeks), as assessed by two psychiatrists, and ≤20% reduction in $HDRS_{17}$ score between the two visits; and (5) current antidepressant or psychotropic

medication regimen had to be stable for at least 4 weeks before study entry. Exclusion criteria included (1) the presence of other psychiatric comorbidities, including obsessive–compulsive disorder, posttraumatic stress disorder, panic disorder, anorexia nervosa, substance use disorder and personality disorder; (2) the presence of central nervous system disease that impairs motor, sensory or cognitive function or that requires intermittent or chronic medication; (3) previous ablative or other intracranial surgery or any medical contraindication to surgery; (4) contraindication to MRI scanning; (5) pregnancy or intent to conceive during the study; and (6) current participation in another investigational device, drug or surgical trial.

The study procedures were approved by the Ethics Committee of the First Medical Center, General Hospital of the Chinese People's Liberation Army, Shenzhen Second People's Hospital and Shenzhen Kangning Hospital. Patients and their legal guardians were fully informed of the therapy and signed the informed consent, according to case report guidelines and in compliance with the Declaration of Helsinki principles. The DBS system is provided free of charge to patients in our study. This trial was registered under the clinical trial numbers NCT03667872 and ChiCTR2100045363.

DBS surgery

For each patient, a safe frontal trajectory for the left and right Hb was planned by preoperative MRI co-fused with computed tomography (CT) using the Leksell stereotactic frame (Elekta). All patients underwent implantation of DBS electrodes with four 1.5 mm contacts separated by 0.5 mm (L301C, PINS) under general anesthesia (Fig. 1d). Two electrodes were implanted bilaterally into the Hb, and an LFP sensing-enabled neurostimulator (G102RS, PINS) was connected to the leads (E202C, PINS). Intraoperative MRI and postoperative CT scans were conducted within 24 h to ensure successful implantation and to rule out any surgery-related complications, such as intracranial pneumatosis or intracerebral hemorrhage.

DBS electrodes localization

The locations of the DBS electrodes were reconstructed with Lead-DBS 2.5 (ref. 40). The 1-month postoperative CT was coregistered to the preoperative T1-weighted MRI using advanced normalization tools and then normalized to the Montreal Neurological Institute (MNI) space. The Hb was defined according to the DBS Tractography Atlas provided by Lead-DBS. The patient's implanted DBS electrodes are displayed in Fig. 1b and Supplementary Fig. 1.

Clinical evaluation and follow-up

One psychiatrist blinded to the current stimulus parameters evaluated clinical efficacy using the $HDRS_{17}$ and the HARS at baseline (that is, preoperative scores) and monthly after surgery for 6 months. Another physician was responsible for regulating the therapeutic contacts (monopolar stimulation) and parameters. First, based on the optimum position of electrode contacts, an individualized recommended stimulation voltage was determined for each patient using the SimBio/FieldTrip model through Lead-DBS version 2.2.0 (ref. 40) (Supplementary Fig. 1). Second, at month 0 (Fig. 1c), the physician conducted a program test to identify the stimulation voltage range and the best therapeutic voltage for each patient. The DBS was continuously applied throughout the 6-month treatment, and the therapeutic contact and voltage of Hb were adjusted based on each patient's clinical response. Patients were permitted to maintain or reduce their previous medications during the 6-month follow-up period, unless an intervention was required.

LFP data acquisition

The LFPs were recorded by the LFP sensing-enabled neurostimulator and transmitted to an external computer equipped with a telemetry head for high-speed decoding, real-time display and storage[41–44]. During the recording period, the DBS system functioned normally in each patient, with particular attention paid to wireless communication and impedance (Fig. 1a). To reduce electrocardiographic signals from the LFP signal recording, the bipolar stimulation mode was utilized[45]. A sampling rate of 500 Hz was used for DBS off and on recordings (5 min each, using the same contacts). The LFP signals were preprocessed using a hardware-based 0.3 Hz high-pass filter and a 250 Hz low-pass filter.

MRI data acquisition

Both preoperative and postoperative structural and functional MRI (fMRI) images were acquired with a 3.0 T Prisma (Siemens) MRI scanner equipped with a 64-channel head coil. Structural images were acquired using a sagittal magnetization-prepared rapid gradient echo T1-weighted sequence (0.7-mm isotropic resolution, field of view (FOV) of 224, FOV phase of 100%, slice thickness of 0.7 mm, repetition time of 2,200 ms, echo time of 2.48 ms and flip angle of 8°). Functional images were acquired using an echo-planar imaging sequence (voxel size of 3.0 × 3.0 × 3.0 mm, FOV of 216, FOV phase of 100%, slice thickness of 3.0 mm, repetition time of 3,000 ms, echo time of 30 ms and flip angle of 85°).

At month 0, each patient underwent one structural MRI and six fMRI runs, with each run lasting 5 min and 17 s. The first three runs were conducted without stimulation, while the next three were performed with the treatment parameters activated. Patients were instructed to keep their eyes closed and remain relaxed during the scans without falling asleep. The safety of the DBS system in 3.0 T MRI was demonstrated in our previous study[38,46,47].

LFP analysis

For the LFP data, the first 1-s segment was excluded due to unstable pulse generator activity immediately following DBS activation. To reduce baseline drift and stimulation artifacts, a 2–100 Hz bandpass filter and customized trap filters were applied to the remaining segments, as described in previous studies[45,48]. Segments with substantial movement artifacts were excluded from subsequent data analyses. The PSD of LFPs was estimated by Welch's method with a frequency resolution of 0.1 Hz and then normalized (a.n.) by dividing the total power between 2 Hz and 30 Hz. Power was calculated as the sum of the relative normalized PSD in each band (delta band, 2–4 Hz; theta band, 4–8 Hz; alpha band, 8–13 Hz; beta band, 14–30 Hz). The difference in power between DBS on and off at session 0 was calculated for each band.

fMRI analysis

The fMRI data were preprocessed using SPM12 (http://www.fil.ion.ucl.ac.uk/spm/) and custom codes written in MATLAB. First, the functional images were corrected with the middle slice serving as a reference to adjust for timing differences in slice acquisition and were realigned to the first scan via rigid-body motion correction. Then, the T1 images of patients were spatially coregistered to their mean fMRI image, followed by spatial coregistration and normalization to the standard stereotactic MNI space. The functional images were also normalized to the MNI space (resampled voxel size of $3 \times 3 \times 3\ mm^3$) using the coregistration parameters of the T1 image and were spatially smoothed with a 4-mm full width at half maximum Gaussian kernel. Finally, the effects of white matter, cerebrospinal fluid, head motion (Friston-24 motion parameters) and linear trends were removed from the fMRI time courses.

To obtain voxel-wise fALFF maps, the preprocessed fMRI time courses first underwent a transformation to the frequency domain using a fast Fourier transform, followed by the calculation of the power spectrum. Then, the fALFF value for each voxel was obtained by calculating the ratio of the power spectrum within the predefined frequency band (0.01–0.10 Hz) to that of the entire frequency range (0–0.167 Hz)[49].

Further, we selected brain regions that were closely associated with reward circuits from Anatomical Atlas Labelling version 3 (https://www.oxcns.org/aal3.html), including bilateral mOFC, bilateral lateral

orbital gyrus, bilateral putamen, bilateral NAc, VTA, SNc and raphe. The fALFF of each brain region was calculated by averaging the voxel-wise fALFF values within that region when DBS was turned on and off at month 0, respectively.

Statistical analysis

The Wilcoxon matched-pairs signed rank test was used to compare the patients' scores on the $HDRS_{17}$ and HARS obtained at baseline with their corresponding scores obtained at 1-, 3- and 6-month follow-ups, the LFP in the left and right Hb, as well as region-wise fALFF when DBS was turned on and off at month 0. The significance level for all tests was set at 0.05 (two sided). We presented data as mean ± standard deviation, and included individual patient data along with the group-averaged data and corresponding statistical results to present inter-individual differences in clinical and neural responses using GraphPad Prism 8.0. It is worth noting that the efficacy of patient 1 had been reported in previous literature[25].

Reporting summary

Further information on research design is available in the Nature Portfolio Reporting Summary linked to this article.

Data availability

All data generated or analyzed are included in the manuscript and supporting files. Source data are provided with this paper.

Code availability

The publicly available software and code for the analysis has been described in Methods of our manuscript. The code for LFP analysis can be accessed at https://github.com/nercnlab/LFP-analysis/blob/main/Num_LFP%20analysis (ref. 50).

References

1. Dandekar, M. P. et al. Deep brain stimulation for treatment-resistant depression: an integrative review of preclinical and clinical findings and translational implications. *Mol. Psychiatry* **23**, 1094–1112 (2018).
2. Hitti, F. L. et al. Deep brain stimulation is effective for treatment-resistant depression: a meta-analysis and meta-regression. *J. Clin. Med.* **9**, 2796 (2020).
3. Holtzheimer, P. E. et al. Subcallosal cingulate deep brain stimulation for treatment-resistant depression: a multisite, randomised, sham-controlled trial. *Lancet Psychiatry* **4**, 839–849 (2017).
4. Coenen, V. A. et al. Superolateral medial forebrain bundle deep brain stimulation in major depression: a gateway trial. *Neuropsychopharmacology* **44**, 1224–1232 (2019).
5. Bergfeld, I. O. et al. Deep brain stimulation of the ventral anterior limb of the internal capsule for treatment-resistant depression: a randomized clinical trial. *JAMA Psychiatry* **73**, 456–464 (2016).
6. Dougherty, D. D. et al. A randomized sham-controlled trial of deep brain stimulation of the ventral capsule/ventral striatum for chronic treatment-resistant depression. *Biol. Psychiatry* **78**, 240–248 (2015).
7. Voineskos, D., Daskalakis, Z. J. & Blumberger, D. M. Management of treatment-resistant depression: challenges and strategies. *Neuropsychiatr. Dis. Treat.* **16**, 221–234 (2020).
8. Abraham, M. E. et al. Investigating deep brain stimulation of the habenula: a review of clinical studies. *Neuromodulation* **26**, 292–301 (2023).
9. Germann, J. et al. Deep brain stimulation of the habenula: systematic review of the literature and clinical trial registries. *Front. Psychiatry* **12**, 730931 (2021).
10. Proulx, C. D., Hikosaka, O. & Malinow, R. Reward processing by the lateral habenula in normal and depressive behaviors. *Nat. Neurosci.* **17**, 1146–1152 (2014).
11. Fakhoury, M. The habenula in psychiatric disorders: more than three decades of translational investigation. *Neurosci. Biobehav. Rev.* **83**, 721–735 (2017).
12. Yang, Y. et al. Lateral habenula in the pathophysiology of depression. *Curr. Opin. Neurobiol.* **48**, 90–96 (2018).
13. Matsumoto, M. & Hikosaka, O. Lateral habenula as a source of negative reward signals in dopamine neurons. *Nature* **447**, 1111–1115 (2007).
14. Matsumoto, M. & Hikosaka, O. Two types of dopamine neuron distinctly convey positive and negative motivational signals. *Nature* **459**, 837–841 (2009).
15. Hu, H., Cui, Y. & Yang, Y. Circuits and functions of the lateral habenula in health and in disease. *Nat. Rev. Neurosci.* **21**, 277–295 (2020).
16. Beier, K. T. et al. Circuit architecture of VTA dopamine neurons revealed by systematic input-output mapping. *Cell* **162**, 622–634 (2015).
17. Ren, J. et al. Anatomically defined and functionally distinct dorsal raphe serotonin subsystems. *Cell* **175**, 472–487.e20 (2018).
18. Cerniauskas, I. et al. Chronic stress induces activity, synaptic, and transcriptional remodeling of the lateral habenula associated with deficits in motivated behaviors. *Neuron* **104**, 899–915.e8 (2019).
19. Foster, S. et al. Abnormal habenula functional connectivity characterizes treatment-resistant depression. *Neuroimage Clin.* **34**, 102990 (2022).
20. Yang, Y. et al. Ketamine blocks bursting in the lateral habenula to rapidly relieve depression. *Nature* **554**, 317–322 (2018).
21. Morris, J. S. et al. Covariation of activity in habenula and dorsal raphé nuclei following tryptophan depletion. *Neuroimage* **10**, 163–172 (1999).
22. Schmidt, F. M. et al. Habenula volume increases with disease severity in unmedicated major depressive disorder as revealed by 7T MRI. *Eur. Arch. Psychiatry Clin. Neurosci.* **267**, 107–115 (2017).
23. Sartorius, A. et al. Remission of major depression under deep brain stimulation of the lateral habenula in a therapy-refractory patient. *Biol. Psychiatry* **67**, e9–e11 (2010).
24. Zhang, C. et al. Bilateral habenula deep brain stimulation for treatment-resistant depression: clinical findings and electrophysiological features. *Transl. Psychiatry* **12**, 52 (2022).
25. Wang, Z. et al. Case report: lateral habenula deep brain stimulation for treatment-resistant depression. *Front. Psychiatry* **11**, 616501 (2021).
26. Cui, Z. et al. Safety and precision of frontal trajectory of lateral habenula deep brain stimulation surgery in treatment-resistant depression. *Front. Neurol* **14**, 1113545 (2023).
27. Mayberg, H. S. et al. Deep brain stimulation for treatment-resistant depression. *Neuron* **45**, 651–660 (2005).
28. Fenoy, A. J. et al. A longitudinal study on deep brain stimulation of the medial forebrain bundle for treatment-resistant depression. *Transl. Psychiatry* **8**, 111 (2018).
29. Zhang, Y. et al. Deep brain stimulation in the lateral habenula reverses local neuronal hyperactivity and ameliorates depression-like behaviors in rats. *Neurobiol. Dis.* **180**, 106069 (2023).
30. Amo, R. et al. Identification of the zebrafish ventral habenula as a homolog of the mammalian lateral habenula. *J. Neurosci.* **30**, 1566–1574 (2010).
31. Lawson, R. P. et al. The habenula encodes negative motivational value associated with primary punishment in humans. *Proc. Natl Acad. Sci. USA* **111**, 11858–11863 (2014).
32. Ahumada-Galleguillos, P. et al. Directional asymmetry in the volume of the human habenula. *Brain Struct. Funct.* **222**, 1087–1092 (2017).
33. Barreiros, A. R. et al. Abnormal habenula functional connectivity characterizes treatment-resistant depression. *Neuroimage Clin.* **34**, 102990 (2022).

34. Hu, H. Reward and aversion. *Annu. Rev. Neurosci.* **39**, 297–324 (2016).
35. Lin, S. et al. The ATP level in the medial prefrontal cortex regulates depressive-like behavior via the medial prefrontal cortex–lateral Habenula pathway. *Biol. Psychiatry* **92**, 179–192 (2022).
36. Fan, Z. et al. Neural mechanism underlying depressive-like state associated with social status loss. *Cell* **186**, 560–576.e17 (2023).
37. Li, G. et al. Instantaneous antidepressant effect of lateral habenula deep brain stimulation in rats studied with functional MRI. *eLife* **12**, e84693 (2023).
38. Shen, L. et al. Subthalamic nucleus deep brain stimulation modulates 2 distinct neurocircuits. *Ann. Neurol.* **88**, 1178–1193 (2020).
39. Min, H. K. et al. Deep brain stimulation induces BOLD activation in motor and non-motor networks: an fMRI comparison study of STN and EN/GPi DBS in large animals. *Neuroimage* **63**, 1408–1420 (2012).
40. Horn, A. et al. Lead-DBS v2: towards a comprehensive pipeline for deep brain stimulation imaging. *Neuroimage* **184**, 293–316 (2019).
41. Qian, X. et al. A method for removal of deep brain stimulation artifact from local field potentials. *IEEE Trans. Neural Syst. Rehabil. Eng.* **25**, 2217–2226 (2017).
42. Qian, X. et al. Chronically monitoring the deep brain rhythms: from stimulation to recording. *Sci. Bull.* **61**, 1522–1524 (2016).
43. Ding, J. Q. et al. Role of MRI coils in radio frequency heating of implantable medical devices. *Electron. Lett.* **54**, 682–683 (2018).
44. Zhang, F. et al. Safety assessment of displacement force, torque and vibration of a deep brain stimulation system under 3T MRI. *Int. J. Appl. Electromagnet. Mech.* **59**, 1081–1086 (2019).
45. Chen, Y. et al. Neuromodulation effects of deep brain stimulation on beta rhythm: a longitudinal local field potential study. *Brain Stimul.* **13**, 1784–1792 (2020).
46. Wan, S. et al. Evaluation of local B1 field as dosimeter of RF heating for implant in MRI. *Electron. Lett.* **55**, 302–304 (2019).
47. Qian, X. et al. A platform for long-term monitoring the deep brain rhythms. *Exp. Neurol.* **294**, 68–77 (2017).
48. Keshtkaran, M. R. & Yang, Z. A fast, robust algorithm for power line interference cancellation in neural recording. *J. Neural Eng.* **11**, 026017 (2014).
49. Zou, Q. H. et al. An improved approach to detection of amplitude of low-frequency fluctuation (ALFF) for resting-state fMRI: fractional ALFF. *J. Neurosci. Methods* **172**, 137–141 (2008).
50. nercnlab / LFP-analysis. *GitHub* https://github.com/nercnlab/LFP-analysis/blob/main/Num_LFP%20analysis (2024).

Acknowledgements

We thank Q. Cui and Y. Tian at the National Engineering Research Center of Neuromodulation for assistance in the reconstruction of implanted DBS images. We also thank Beijing PINS Medical Equipment Co., Ltd. for donating the most cutting-edge DBS systems. This work was supported by the Scientific Foundation of Institute of Psychology, Chinese Academy of Sciences (E2CX6515, Z.W.), the National Key Research and Development Program of China (2019YFC0118503, Z.C.), the Shenzhen International Cooperative Research Project (GJHZ20180930110402104, L.L.) and the National Natural Science Foundation of China (82101549, Z.W.).

Author contributions

Z.W.: conceptualization, data curation, formal analysis, funding acquisition, investigation, methodology, project administration, visualization, writing—original draft, writing—review and editing. C.J.: data curation, investigation, methodology, writing—original draft. L.G.: data curation, investigation, methodology, software, writing—original draft. L.Z.: formal analysis, methodology, software, visualization, writing—original draft. T.F.: conceptualization, data curation, methodology, supervision. J.W.: data curation, methodology. X.C.: data curation, methodology, supervision. Y.Z.: data curation, methodology, supervision. C.Y.: data curation, methodology. B.P.: data curation, methodology. F.W.: visualization. C.H.: funding acquisition, project administration. Z.C.: conceptualization, data curation, funding acquisition, project administration, resources, supervision, writing—review and editing. Y.T.: formal analysis, methodology, visualization, writing—original draft, writing—review and editing. L.L.: conceptualization, funding acquisition, resources, supervision, writing—review and editing.

Competing interests

All authors declare no competing interests.

Additional information

Supplementary information The online version contains supplementary material available at https://doi.org/10.1038/s44220-024-00286-2.

Correspondence and requests for materials should be addressed to Zhiqiang Cui, Yiheng Tu or Luming Li.

Peer review information *Nature Mental Health* thanks Jürgen Germann and the other, anonymous reviewer(s) for their contribution to the peer review of this work.

Reprints and permissions information is available at www.nature.com/reprints.

Publisher's note Springer Nature remains neutral with regard to jurisdictional claims in published maps and institutional affiliations.

[1]CAS Key Laboratory of Mental Health, Institute of Psychology, Chinese Academy of Sciences, Beijing, China. [2]Department of Psychology, University of Chinese Academy of Sciences, Beijing, China. [3]National Engineering Research Center of Neuromodulation, School of Aerospace Engineering, Tsinghua University, Beijing, China. [4]Department of Neurosurgery, Chinese People's Liberation Army of China General Hospital, Beijing, China. [5]Peking University Institute of Mental Health, National Health Commission Key Laboratory of Mental Health, Peking University, National Clinical Research Center for Mental Disorders, Peking University Six Hospital, Beijing, China. [6]Department of Neurosurgery, Shenzhen Second People's Hospital, The First Affiliated Hospital of Shenzhen University, Shenzhen, China. [7]Department of Depressive Disorder, Shenzhen Mental Health Center, Shenzhen, China. [8]IDG/McGovern Institute for Brain Research, Tsinghua University, Beijing, China. ✉e-mail: zhiqiangcui2008@hotmail.com; yihengtu@gmail.com; lilm@tsinghua.edu.cn

nature portfolio

Corresponding author(s): Zhiqiang Cui, Yiheng Tu, Luming Li

Last updated by author(s): Zhiqiang Cui, Yiheng Tu, Luming Li
April 21st, 2024

Reporting Summary

Nature Portfolio wishes to improve the reproducibility of the work that we publish. This form provides structure for consistency and transparency in reporting. For further information on Nature Portfolio policies, see our Editorial Policies and the Editorial Policy Checklist.

Please do not complete any field with "not applicable" or n/a. Refer to the help text for what text to use if an item is not relevant to your study.
For final submission: please carefully check your responses for accuracy; you will not be able to make changes later.

Statistics

For all statistical analyses, confirm that the following items are present in the figure legend, table legend, main text, or Methods section.

n/a	Confirmed	
☐	☑	The exact sample size (*n*) for each experimental group/condition, given as a discrete number and unit of measurement
☐	☑	A statement on whether measurements were taken from distinct samples or whether the same sample was measured repeatedly
☐	☑	The statistical test(s) used AND whether they are one- or two-sided *Only common tests should be described solely by name; describe more complex techniques in the Methods section.*
☐	☑	A description of all covariates tested
☐	☑	A description of any assumptions or corrections, such as tests of normality and adjustment for multiple comparisons
☐	☑	A full description of the statistical parameters including central tendency (e.g. means) or other basic estimates (e.g. regression coefficient) AND variation (e.g. standard deviation) or associated estimates of uncertainty (e.g. confidence intervals)
☐	☑	For null hypothesis testing, the test statistic (e.g. *F*, *t*, *r*) with confidence intervals, effect sizes, degrees of freedom and *P* value noted *Give P values as exact values whenever suitable.*
☑	☐	For Bayesian analysis, information on the choice of priors and Markov chain Monte Carlo settings
☑	☐	For hierarchical and complex designs, identification of the appropriate level for tests and full reporting of outcomes
☐	☑	Estimates of effect sizes (e.g. Cohen's *d*, Pearson's *r*), indicating how they were calculated

Our web collection on statistics for biologists contains articles on many of the points above.

Software and code

Policy information about availability of computer code

Data collection	No software was used to collect clinical data. The local field potential (LFP) data was colleated using the deep brain stimulation (DBS) system which was enabled wireless collection of LFP signals and the functional magnetic resonance imaging (fMRI) data was collected using 3.0T Prisma (SIEMENS) MRI scanner.
Data analysis	The publicly available software (GraphPad Prisma 8.0, SPM 12.0 and Matlab2021b) and code (Matlab) for the analysis has been described in the Methods of our manuscript.

For manuscripts utilizing custom algorithms or software that are central to the research but not yet described in published literature, software must be made available to editors and reviewers. We strongly encourage code deposition in a community repository (e.g. GitHub). See the Nature Portfolio guidelines for submitting code & software for further information.

Data

Policy information about availability of data

All manuscripts must include a data availability statement. This statement should provide the following information, where applicable:

- Accession codes, unique identifiers, or web links for publicly available datasets
- A description of any restrictions on data availability
- For clinical datasets or third party data, please ensure that the statement adheres to our policy

All data used to generated or analysed is provided in the manuscript and supporting files.

Research involving human participants, their data, or biological material

Policy information about studies with human participants or human data. See also policy information about sex, gender (identity/presentation), and sexual orientation and race, ethnicity and racism.

Reporting on sex and gender	The study included 4 males and 2 females.
Reporting on race, ethnicity, or other socially relevant groupings	The study included six Chinese patients with treatment-resistent depression (TRD).
Population characteristics	The six patients with TRD included five unipolar and one bipolar. They had an average age of 26.67 (Patient 1-6: 34, 30, 22, 34, 18 and 22).
Recruitment	In this study, patients were recruited by advertisements in hospitals. After being assessed by professional psychiatrists to met the inclusion and exclusion criteria and with the full informed consent of patients and their families, the patients with TRD were enrolled voluntarily.
Ethics oversight	The study procedures were approved by the Ethics Committee of First Medical Center, General Hospital of the Chinese People's Liberation Army, Shenzhen Second People's Hospital and Shenzhen Kangning Hospital.

Note that full information on the approval of the study protocol must also be provided in the manuscript.

Field-specific reporting

Please select the one below that is the best fit for your research. If you are not sure, read the appropriate sections before making your selection.

☑ Life sciences ☐ Behavioural & social sciences ☐ Ecological, evolutionary & environmental sciences

For a reference copy of the document with all sections, see nature.com/documents/nr-reporting-summary-flat.pdf

Life sciences study design

All studies must disclose on these points even when the disclosure is negative.

Sample size	This is a prospective, case series, open-label clinical study. The sample size is not pre-designed.
Data exclusions	Patient 6 withdraw from the study at 3-month follow up for her unwilling to continue the following follow-ups and the LFP of patient 1 excluded from the analysis because of the short data duration with DBS turned on.
Replication	This study is an individualized longitudinal study. The efficacy of DBS treatment and data collected from each patient are not reproducible. Therefore, additional clinical studies are required to validate the findings.
Randomization	The study did not involved randomization. Randomization requires a certain sample size, and the sample size of this study is 6. Moreover, we aimed to investigate the efficacy and neural mechanism of Hb DBS for TRD through a small sample size of patients, providing a basis for subsequent randomized clinical studies.
Blinding	In our study, the physician who assessed the $HDRS_{17}$ and person who collected the physiological signals from patients were blinded.

Behavioural & social sciences study design

All studies must disclose on these points even when the disclosure is negative.

Study description	
Research sample	
Sampling strategy	
Data collection	
Timing	
Data exclusions	
Non-participation	
Randomization	

Ecological, evolutionary & environmental sciences study design

All studies must disclose on these points even when the disclosure is negative.

Study description	
Research sample	
Sampling strategy	
Data collection	
Timing and spatial scale	
Data exclusions	
Reproducibility	
Randomization	
Blinding	

Did the study involve field work? ☐ Yes ☐ No

Field work, collection and transport

Field conditions	
Location	
Access & import/export	
Disturbance	

Reporting for specific materials, systems and methods

We require information from authors about some types of materials, experimental systems and methods used in many studies. Here, indicate whether each material, system or method listed is relevant to your study. If you are not sure if a list item applies to your research, read the appropriate section before selecting a response.

Materials & experimental systems

n/a	Involved in the study
☑	☐ Antibodies
☑	☐ Eukaryotic cell lines
☑	☐ Palaeontology and archaeology
☑	☐ Animals and other organisms
☐	☑ Clinical data
☑	☐ Dual use research of concern
☑	☐ Plants

Methods

n/a	Involved in the study
☑	☐ ChIP-seq
☑	☐ Flow cytometry
☐	☑ MRI-based neuroimaging

Antibodies

Antibodies used	
Validation	

Eukaryotic cell lines

Policy information about cell lines and Sex and Gender in Research

Cell line source(s)	
Authentication	
Mycoplasma contamination	
Commonly misidentified lines (See ICLAC register)	

Palaeontology and Archaeology

Specimen provenance	
Specimen deposition	
Dating methods	

☐ Tick this box to confirm that the raw and calibrated dates are available in the paper or in Supplementary Information.

Ethics oversight	

Note that full information on the approval of the study protocol must also be provided in the manuscript.

Animals and other research organisms

Policy information about studies involving animals; ARRIVE guidelines recommended for reporting animal research, and Sex and Gender in Research

Laboratory animals	
Wild animals	
Reporting on sex	
Field-collected samples	
Ethics oversight	

Note that full information on the approval of the study protocol must also be provided in the manuscript.

Clinical data

Policy information about clinical studies

All manuscripts should comply with the ICMJE guidelines for publication of clinical research and a completed CONSORT checklist must be included with all submissions.

Clinical trial registration	The study was registered at www.clinicaltrial.gov (NCT03667872) and www.chictr.org.cn/index.aspx (ChiCTR2100045363), respectively.
Study protocol	The study was a prospective, open-label clinical study. Six TRD patients were recruited from two clinical centers. The detailed study protocol can be found in the Methods section.
Data collection	The clinial data was collected at baseline, 1-,3- and 6-month follow-ups.The LFP and fMRI data were collected at month 0. The detailed study protocol can be found in the Methods section.
Outcomes	The primary outcome was the reduction of 17-item Hamilton Depression Rating Scale ($HDRS_{17}$) scores compared to baseline. The secondary outcomes was the reduction of Hamilton Anxiety Rating Scale (HARS) scores compared to baseline.

Dual use research of concern

Policy information about dual use research of concern

Hazards

Could the accidental, deliberate or reckless misuse of agents or technologies generated in the work, or the application of information presented in the manuscript, pose a threat to:

No	Yes	
☐	☐	Public health
☐	☐	National security
☐	☐	Crops and/or livestock
☐	☐	Ecosystems
☐	☐	Any other significant area

Experiments of concern

Does the work involve any of these experiments of concern:

No	Yes	
☐	☐	Demonstrate how to render a vaccine ineffective
☐	☐	Confer resistance to therapeutically useful antibiotics or antiviral agents
☐	☐	Enhance the virulence of a pathogen or render a nonpathogen virulent
☐	☐	Increase transmissibility of a pathogen
☐	☐	Alter the host range of a pathogen
☐	☐	Enable evasion of diagnostic/detection modalities
☐	☐	Enable the weaponization of a biological agent or toxin
☐	☐	Any other potentially harmful combination of experiments and agents

Plants

Seed stocks

Novel plant genotypes

Authentication

ChIP-seq

Data deposition

☐ Confirm that both raw and final processed data have been deposited in a public database such as GEO.

☐ Confirm that you have deposited or provided access to graph files (e.g. BED files) for the called peaks.

Data access links
May remain private before publication.

Files in database submission

Genome browser session
(e.g. UCSC)

Methodology

Replicates

Sequencing depth

Antibodies

Peak calling parameters

Data quality

Software

Flow Cytometry

Plots

Confirm that:

☐ The axis labels state the marker and fluorochrome used (e.g. CD4-FITC).

☐ The axis scales are clearly visible. Include numbers along axes only for bottom left plot of group (a 'group' is an analysis of identical markers).

☐ All plots are contour plots with outliers or pseudocolor plots.

☐ A numerical value for number of cells or percentage (with statistics) is provided.

Methodology

Sample preparation	
Instrument	
Software	
Cell population abundance	
Gating strategy	

☐ Tick this box to confirm that a figure exemplifying the gating strategy is provided in the Supplementary Information.

Magnetic resonance imaging

Experimental design

Design type	Resting-state functional MRI
Design specifications	Imaging acquisition protocol included 2 modalities. The collection order is T1-weighted structural imaging and resting-state functional imaging.
Behavioral performance measures	Depressive symptoms were measured using $HDRS_{17}$; Anxious symptoms were measured using Hamilton Anxiety Rating Scale (HARS).
Imaging type(s)	Functional imaging
Field strength	3.0T
Sequence & imaging parameters	Functional MRI images were acquired from a 3.0T Prisma MRI scanner using echo-planar imaging sequence with the following parameters：FOV=216mm, slice thickness=3mm, TR=3s, TE=30ms, flip angle=85°
Area of acquisition	Whole brain

Diffusion MRI ☐ Used ☑ Not used

Preprocessing

Preprocessing software	Functional imaging was preprocessed using SPM12.0.
Normalization	The normalization was performed in SPM12.0 using non-linear registration.
Normalization template	The data were normalized to the MNI152 atlas.
Noise and artifact removal	The head motion was corrected using rigid body correction; The signals of white matter and cerebrospinal fluid, Friston-24 motion parameters, and linear trends were regressed.
Volume censoring	No volume censoring was performed.

Statistical modeling & inference

Model type and settings	The study is not involved in task MRI and no model was used.
Effect(s) tested	For resting-state fMRI, ROI-wise fALFF were compared between DBS off and on sessions at month 0.

Specify type of analysis: ☐ Whole brain ☑ ROI-based ☐ Both

Statistic type for inference

(See Eklund et al. 2016)

Wilcoxon matched-pairs signed rank test was used for comparison of fALFF.

Correction

No correction

Models & analysis

n/a	Involved in the study
☑	☐ Functional and/or effective connectivity
☑	☐ Graph analysis
☑	☐ Multivariate modeling or predictive analysis

Functional and/or effective connectivity

Graph analysis

Multivariate modeling and predictive analysis